Global Near-Real-Time Estimates of Biomass Burning Emissions using Satellite Active Fire Detections

Jay Al-Saadi
NASA Langley Research Center, Hampton, VA
j.a.al-saadi@nasa.gov

Amber Soja
National Institute of Aerospace, Hampton, VA

Brad Pierce
NASA Langley Research Center, Hampton, VA

Chieko Kittaka
SSAI, Hampton, VA

Louisa Emmons
NCAR, Boulder, CO

Shobha Kondragunta and Xiaoyang Zhang
NOAA NESDIS, Camp Springs, MD

Christine Wiedinmyer
NCAR, Boulder, CO

Todd Schaack
Space Science and Engineering Center, University of Wisconsin, Madison WI

Jim Szykman
US EPA, Research Triangle Park, NC

ABSTRACT

We present a new technique for generating daily global estimates of biomass burning emissions suitable for use in models forecasting atmospheric chemical composition and air quality. We combine ecosystem-dependent carbon fuel databases, fire weather severity estimates, and near-real-time satellite fire detections from the MODIS instruments to estimate the amount of carbon released from active fires. Emissions of CO, NOx, and hydrocarbons are then estimated using ecosystem-dependent emission ratios. These emissions estimates have been used to provide global chemical and regional aerosol forecasts for much of 2006 using the NASA/University of Wisconsin Realtime Air Quality Modeling System (RAQMS). The largest overall uncertainty in this approach lies in inferring area burned from instantaneous active fire detections. Here we evaluate emissions for spring and summer of 2006 by intercomparing our emissions estimates with three other approaches using satellite fire detections over regional to global domains: 1) NOAA GOES fire detections over the continental US, 2) MODIS fire and landcover products over North and Central America, and 3) 8-day composite MODIS detections applied to global GFEDv2 emissions. Overall we find there are large differences in area-burned estimates, particularly for small fires. We compare RAQMS global CO predictions with observations from the MOPITT and TES instruments over regions where biomass burning is significant. CO emission estimates from burning are consistent with satellite observations over the US but we find large discrepancy in three out of four regions of large tropical burning.

INTRODUCTION

Biomass burning is a major contributor of particulate matter and trace gases to the global troposphere. Burning is also subject to large interannual variability [van der Werf et al., 2006]. Together these two facts define both the fundamental importance of and difficulty in establishing accurate biomass burning emissions inventories. The problem is further compounded by differing temporal and spatial requirements. Air quality modeling at the regional and local level requires that emissions be resolved at diurnal or even hourly scales. Further, large fires are capable of lofting emissions into the upper troposphere, where strong winds can result in inter-regional and intercontinental transport of these emissions within a few days. In these situations there is potential for local air quality to be significantly influenced by events outside the domain of regional air quality models.

An approach for addressing this variability in biomass burning emissions is to calculate spatially and temporally accurate emissions based on observations of active fires. Satellite observations provide a consistent means of detecting active burning at continental to global scales. Geostationary platforms, such as the NOAA GOES satellites, can provide continuous observations over regional domains, making it possible to detect short duration fires and also to resolve diurnal behavior of large fires. Polar orbiting satellites, including the NASA Terra and Aqua satellites, can provide global coverage but typically at only once per day.

Here we begin to assess the uncertainties in current biomass emission estimates constrained by active satellite fire detections. We first introduce a new technique for generating daily global biomass burning emissions estimates in near real time for use in atmospheric composition forecasts. We then intercompare 2006 estimates of area burned and biomass burning CO emissions generated from four different methods using active satellite fire detections from both polar-orbiting and geostationary satellites. We also evaluate the CO emissions by comparing model predictions with satellite observations and aircraft in-situ data in regions where biomass burning is significant. Most of the analysis focuses on the continental US (CONUS) where the product based on geostationary GOES observations is available. Our intent is to better understand the factors controlling biomass burning emissions over CONUS and to apply this insight to other regions of the globe.

BIOMASS BURNING EMISSIONS TECHNIQUES

In this paper we compare four different techniques that use satellite active fire detections to produce emissions estimates. The techniques are summarized in Table 1. Two of the techniques are global and two are regional. Both global techniques use MODIS fire detections although at different levels of processing. One regional technique uses MODIS detections and one uses processed GOES detections. The newly technique used in the NASA/University of Wisconsin Realtime Air Quality Modeling System (RAQMS) [Pierce et al., 2003; Kittaka et al., 2004; Pierce et al., 2006] is described in some detail, while the three other emissions techniques have each been described in the literature so only very brief summaries are given here.

RAQMS Emissions

The new technique described here was developed to provide daily emissions for RAQMS forecasts that were used to support flight planning and data analysis during the March-May 2006 NASA INTEX-B and August-October 2006 NOAA TexAQS field campaigns. These forecasts were also used as lateral boundary conditions for regional air quality predictions with the University of Iowa STEM model [Tang et al., 2007], demonstrating a capability for global-to-regional assessment of burning influences on air quality.

The basic approach [Soja et al., 2007b] relies on gridded carbon fuel consumption databases, satellite fire detections, and meteorology-based estimates of fire weather severity. The ecosystem-dependent carbon consumption databases represent the amounts of carbon released from burning of vegetation and sequestered fuel [Olson et al., 1983; Zinke et al., 1986; Soja et al., 2004] and have been

generated for three classes of fire severity (low, medium, high). We estimate fire weather severity using the US Forest Service Haines Index, which considers atmospheric moisture and thermal stability [Haines, 1988]. The Index gives an indication of the potential for the rate of spread of a fire on a given day. We calculate the Index daily over the entire globe using the 6-hourly meteorological analysis (i.e., 00Z, 06Z, 12Z, 18Z) that is closest in time to local noon. We use the high severity carbon consumption database where the Haines Index is 6, medium severity where the Index is 5, and low severity where the Index is 4 or less.

Our need to generate global emissions in all ecosystems in near real time dictates the use of MODIS Rapid Response fire detections for estimating area burned [NASA/University of Maryland, 2002]. Yet there is large uncertainty in inferring area burned from instantaneous active fire detections, and additional sources of uncertainty include missing fire detections (e.g., due to cloud cover), false detections, and multiple detections of the same fire [Giglio, 2007]. We use instantaneous active fire detections from the two MODIS instruments onboard the NASA Terra and Aqua satellites. Each instrument provides one daytime and one nighttime observation of most of the globe at a nominal 1km x 1km horizontal resolution. At present we create separate day and night emissions estimates, using corresponding day and night MODIS detections, to account for diurnal fire behavior. Daily and nightly total direct carbon emissions are then calculated as the product of area burned and the ecosystem- and severity-specific carbon consumption estimates within each 1x1 degree grid cell. Emissions of other species are determined by combining published emission ratios for different ecosystems [Cofer et al., 1991; Andreae and Merlet, 2001].

Due to the orbital characteristics of Terra and Aqua and the swath width (footprint) of the MODIS instruments, locations at equatorial regions may be viewed only once every other day. Conversely, convergence of orbit tracks at high latitudes provides multiple viewing opportunities of mid and high latitudes per day, raising the possibility of multiple detections of the same fire. Combining Terra and Aqua also presents the possibility of multiple detections at all latitudes. We are presently conducting research into ways of processing the active MODIS fire detections to minimize these sampling biases in daily estimates. In the current technique our approach is to consider 48 hours of MODIS Terra and Aqua data, to ensure complete coverage over equatorial regions, and then attempt to identify and remove multiple detections of the same fire (i.e., same nominal 1km x 1km pixel). Each unique fire detection is assumed to correspond to an area burned of 1 km2 except in savannah/grassland ecosystems where an area of 0.75 km2 is assumed. To illustrate the behavior of this approach, Figure 1 shows time series of daily area burned estimates integrated over Africa and the continental US (CONUS) from March 1 through September 30, 2006. Shown are area estimates resulting from summing all Terra and Aqua fire counts during each 24 hour period (black line) and from the current technique (red line). Over Africa the daily sum shows a strong 2-day signature in which the minima result from gaps in satellite coverage while the maxima are apparently enhanced by multiple detections (i.e., Terra and Aqua see some of the same fires). The current technique has filtered much of this 2-day variability associated with biased sampling and has increased the total area burned estimate by about 10%. Over CONUS the largest impact of the current technique is a general reduction in area burned estimates during the peak summer burning season. This is to be expected since much of the burning in late summer is in the northwestern US, which is at high enough latitudes that there is overlap in the MODIS footprint between successive orbits and multiple detections of the same fires are possible.

NCAR Global Emissions

The NCAR Global technique was developed for retrospective (i.e., not forecast) global analyses with the MOZART model. This technique uses the Global Fire Emissions Database version 2 (GFEDv2) emissions and area burned estimates [van der Werf et al., 2006] scaled by MODIS Terra Climate Modeling Grid (CMG) fire detections [Giglio, 2007]. The GFEDv2 emissions climatology was constructed using data from 1997-2004. The MODIS CMG 8-day fire products are gridded statistical summaries of fire detections over 8-day periods and are intended to remove the single-day sampling

artifacts described above. The emission estimates shown here result from scaling the GFEDv2 inventory by the ratio of 2006 to climatological values of Terra CMG detections at a horizontal resolution of 1x1 degrees.

NCAR Regional Emissions

The NCAR Regional technique was developed to provide high spatial resolution emissions at a daily temporal resolution over a domain including all of North and Central America [Wiedinmyer et al., 2006]. The emissions have been used in forecasts conducted with the WRF-chem model in support of the 2006 Milagro/INTEX field campaigns. Emission estimates are generated for every active fire detection from MODIS Terra and Aqua. Area burned is assumed to be the fraction of each nominal 1 km2 pixel that is vegetated. Ecosystem dependent biomass fuel loading databases, MODIS vegetation products, and published emission ratios are used in deriving the emissions of several trace gases and particulates.

NOAA GOES Emissions

The NOAA GOES emissions rely on Wild Fire Automated Biomass Burning Algorithm (WF_ABBA) instantaneous fire detections [Prins et al., 2003; University of Wisconsin, 2003]. Fire detections are processed every half hour at the nominal horizontal resolution of 4km x 4km. Each detection is assigned a fire flag value from 0 to 5 to indicate details such as confidence, cloud contamination, and sub-pixel processing. For about one third of the fire detections (flag value 0) the processing algorithm can calculate sub-pixel fire characteristics including estimation of instantaneous fire size [Zhang and Kondragunta, 2006a] and recent work has focused on deriving area burned estimates for the remainder of high-confidence detections. Emission estimates are calculated from fuel loading databases [Zhang and Kondragunta, 2006b], combustion efficiency parameters, and emission factors from the First Order Fire Effects Model (FOFEM).

RESULTS

We analyze two of the basic products common to each of the techniques: area burned and CO emissions. For all results shown here the area burned and emission estimates from the two regional models have been aggregated from their native resolutions (1 kmx1km NCAR Regional, 4kmx4km NOAA GOES) to a 1x1 degree grid.

Comparison of techniques over CONUS

Figure 2 shows monthly estimates from each of the techniques integrated over the continental United States during 2006. Within any particular month there is up to an order of magnitude spread in the area burned (top panel) and CO emission (middle panel) estimates The three methods using MODIS fire detections have consistent relationships with each other for both area burned and CO emission in that values from NCAR Regional are largest of the three and from NCAR Global are smallest of the three. These characteristics appear consistent with the treatment of detections. NCAR Regional accumulates all Terra and Aqua detects with no overlap detection and has the largest values. The GFEDv2 database used by NCAR Global uses a regression-tree approach to derive area from fire detections [Giglio et al., 2006] in which a factor of 0.84 km2/pixel was found for temperate North America, versus the nominal factor of 1.0 used by the other 2 methods. RAQMS, with Terra/Aqua overlap detection, yields intermediate values. The GOES technique shows a stronger seasonal cycle in both area burned and CO emission. The area burned estimates are similar to the MODIS-based estimates from May through August and are lower during March, April, and September. GOES-based CO emissions are largest of all techniques from June through September. The bottom panel shows net emission efficiency of carbon, or the ratio of carbon emitted to area burned. In these mean statistics the GOES technique has consistently larger carbon emission efficiency. The MODIS-based approaches show similar emission efficiencies to each other in spite of the different methods for determining CO emissions. Next we focus on two months to analyze details of these comparisons. We look at March, the

period of largest disagreement in both area and CO, and July, a period of good agreement in area burned with large CO emissions and large range of CO emissions.

Figure 3 shows 1-degree maps of area burned from each technique during March 2006. White regions show where no fires were detected. The spatial patterns are reasonably consistent as all methods show that most burning is occurring in the southeastern and south central US and show peak burning in north Texas and the Florida panhandle. GOES has fewer detections in the northern US, particularly the Pacific Northwest. Although the spatial patterns are similar in the southeast, it is clear that the GOES estimates are smaller than the MODIS-based estimates. Much of the burning in the southeast during this time is associated with small-scale agricultural fires and the GOES estimates, based on the half-hourly sub-pixel fire size algorithm, are often smaller than 1km2. Figure 4 shows maps of the CO emissions for March. The CO emissions appear more consistent among the techniques than the area estimates. Largest emissions and largest differences are in the southeast. Shown in Figure 5 are maps of carbon emissions per unit area. Order-of-magnitude differences are apparent in most of the southeast, where GOES values are typically the highest, values from RAQMS and NCAR Regional are quite similar to each other, and values from NCAR Global show much more heterogeneity than the other methods. NCAR Global values in the southeast range from the lowest of all models to among the highest. In the central US the emission efficiency is smaller and is more consistent among the models. Variation in this quantity is highlighting differences in the details of the emission models, including ecosystem and vegetation dependences of emission factors and fuel loadings.

Figure 6 shows maps of area burned in July. The GOES method is detecting more small fires in the Midwest, Plains, and Rocky Mountain regions associated with very small burn areas. All methods appear to produce similar estimates in regions with large area burned (West Coast, Northern Plains). This similarity in the estimates in regions of large area burned leads to the good agreement in overall burned area seen in Figure 2 during July since the totals are dominated by large areas. The CO emissions for July are shown in Figure 7. Again there is good spatial consistency among the techniques as regions of high emissions are similarly captured by all methods. In regions of largest emissions (northwest and southeast) the NCAR Global emissions are smaller than the other methods while in the 1-degree cells with highest emissions the GOES values are typically the largest. July emission per unit area is shown in Figure 8. All methods show high carbon emission efficiencies in the southeast and northwest. Beyond this spatial similarity there is less consistency among the techniques in the actual values of this ratio than was seen in March, although as seen in March the values from the GOES method are larger than the others in high-efficiency regions.

Summary histograms of these 1-degree gridded quantities are considered next. March histograms of area burned, CO emission, and carbon emission ratio are shown in Figure 9. Note that all distributions are shown on a logarithmic scale to capture the wide range of values present. Median values are shown as thin dashed lines. The area-burned distribution from the GOES product has a different shape than the MODIS products, shifted toward smaller values with a median value of 0.15 km2. Median values for the other techniques range from 2.5 km2 for NCAR Global to about 5 km2 for NCAR Regional and RAQMS. The smallest value that can occur in the RAQMS product is 0.75 km2. Both the NCAR Global and NCAR Regional methods have a population of values as small as about 0.3km2. More consistency is found in the histograms of CO emission. Both RAQMS and NCAR Regional have secondary peaks at high emission values while GOES has a relatively broad flat peak. Note that the rightmost portions of the area and CO histograms control the total March values shown in Figure 2. The histograms of carbon emission ratio show that GOES has a distinct population of points with high efficiencies, consistent with the large ratios found in the southeastern US in Figure 5. There is an appearance of bimodality in all four techniques. The high-emission-ratio peak is dominant in GOES and RAQMS, the low-emission-ratio peak is dominant in NCAR Global, and the high- and low-emission-ratio peaks have similar magnitude and are very close together in NCAR Regional. A final note is that these histograms show that overall there are fewer 1-degree cells with fire detections from the GOES product in March.

July histograms are shown in Figure 10. The shapes of the area histograms are more similar in July than in March because the peak in the GOES distribution has shifted to larger values and because all methods show a tail of high values associated with the significant wild fire activity in the Pacific Northwest. The CO emission distributions have similar shapes although the GOES distribution is broader and the RAQMS distribution narrower than the others. The NCAR Global distribution is skewed towards lower CO emissions relative to the other distributions. The carbon efficiencies in July are quite different from those in March. The GOES distribution is still bimodal but the dominant peak occurs at values similar to NCAR Regional and RAQMS. The NCAR Global distribution is the least changed from March to July, having a dominant peak at lower values than the other methods during both months.

We further explore the relationships between CO emission and area burned by considering scatter plots for both months in Figure 11. During March there are two relatively distinct populations apparent in the GOES technique. Within the two populations, CO emissions differ by about an order of magnitude across a wide range of area burned. (This is the cause of the bimodality in the carbon per unit area histograms.) The MODIS-based techniques show a similarly wide range of CO emission values for a given area burned but there are not two distinct populations. Rather, the points are more broadly distributed and shifted toward lower emission efficiencies and larger area burned values, as noted above. During July these relationships are still evident in the scatter plot, but a larger fraction of the GOES points is in the population having lower emission efficiency.

Global comparison of CO emissions

Here we briefly compare global emissions from the two global techniques during months where some of the largest burning is occurring. Figure 12 shows CO emissions from RAQMS and NCAR Global during March 2006. This month was the peak burning in Southeast Asia. Significant burning was also occurring in the tropics of Africa, Central America, and northern South America. While spatial distributions are quite consistent, emission amounts are clearly much larger in RAQMS over Southeast Asia and Africa. Figure 13 shows emissions for August, the month of peak burning in southern subtropical Africa and second largest month for burning in South America. In regions of largest emissions RAQMS is again higher than NCAR Global. These relative characteristics are similar to those found over CONUS, where the RAQMS emission histogram is shifted toward larger values relative to NCAR Global. Much of the difference in the low-latitude regions of large scale burning is associated with different area burned estimates (not shown). In those regions the current 2-day RAQMS technique yields a larger number of detections than the 8-day CMG product. Also, regions evaluated as having high fire weather severity will likely be assigned larger emissions in the RAQMS technique than would result from the climatology-based approach of NCAR Global.

Verification of CO emissions

In this talk we do not evaluate area burned estimates against observations, however Soja et al. [2007a, this issue] evaluate area burned estimates derived from MODIS and GOES fire detections against reported ground-based estimates in Western states. We have recently completed a reanalysis with the RAQMS model, using the biomass burning emissions presented here, in which CO observations from the TES instrument on the Aura satellite have also been assimilated. In regions where CO variability is primarily a result of biomass burning, evaluation of the assimilation increment (assimilation result minus model first guess) provides a measure of the accuracy of the daily RAQMS biomass burning CO emissions used within the assimilation system.

Figure 14 shows net TES-RAQMS CO assimilation increments summed over March and July. The increments are expressed as percentages of the total column amounts and positive values indicate that TES observations have larger CO values than the model first guess. In March the burning emissions are largest in the southeast and Figure 14 shows that first guess CO compares well with TES through much of this region, suggesting that the daily variation and magnitude of the RAQMS burning emissions are realistic. Over Florida and the Gulf Coast the analysis increment is positive (first guess is low relative to

TES), suggesting that the emissions may be underestimated by about 25% in this region. Over north Texas, where all techniques show a local peak in emissions, the analysis increment is negative (first guess is larger than TES), suggesting an overestimate in emissions in that region. During July, when the largest burning emissions are in the west, assimilation increments over burning regions range from zero (northern California, central Oregon) to positive values of about 25% (Washington and Idaho) and 50% and above (Montana), indicating that the RAQMS emissions may have a low bias in the northwest during this time period.

Figure 15 compares CO column amounts from the RAQMS analysis with MOPITT observations during March 2006. Scatter plots of RAQMS versus MOPITT columns are shown over global (lower left panel) and CONUS (lower right panel) domains. Dashed lines show 20% deviations from 1-to-1 lines. Over CONUS the RAQMS analysis is well correlated with MOPITT (r=0.91) but is persistently lower by 20% (mean bias –5.1e17 molec/cm2). During INTEX-B (March-May 2006) it has been shown that the MOPITT column measurements have a mean high bias of 17.9±12.9% (3.6±2.5 e17 molec/cm2) relative to in-situ measurements over North America and the Pacific [Emmons, 2007]. Taken together these evaluations suggest that the RAQMS analysis is consistent with MOPITT observations over CONUS. Globally the mean statistics are also good (r=0.96, mean bias –3.5e17 molec/cm2) but there is a population of points in which the RAQMS CO column is significantly higher than MOPITT. Inspection of the maps (top panels) shows that these points are in the portion of Southeast Asia experiencing large biomass burning, suggesting that the RAQMS burning emissions are too large there. However there is no indication of an overestimate where large burning is occurring over equatorial Africa.

Similar comparisons are presented for August 2006 in Figure 16. Although the overall atmospheric CO column is lower than during March, the correlation and mean bias statistics over CONUS are similar to values in March. Globally there is a much larger population of points where the RAQMS column is significantly larger than MOPITT. The maps show that these points are in the major burning regions of subtropical Africa and South America. These March and August comparisons are consistent with global analyses of the TES-RAQMS assimilation increments (not shown). Overall these evaluations indicate the current RAQMS emission technique is overestimating biomass emissions in 3 out of 4 major tropical burning events by factors of up to 100%. This suggests there is an ecosystem dependence within tropical regions but at this time we have not determined whether this is due to biases in area burned estimates (fire detection issue) or fuel/emission data.

CONCLUSION

We have analyzed area burned and CO emission estimates resulting from four different techniques that use satellite fire detections to constrain area burned. The analysis is primarily focused on the continental U.S. but we also examine global estimates to analyze a wider range of parameters important in characterizing burning emissions. Our primary findings are summarized as follows.

1. Over CONUS there is a wide spread in area burned estimates with a significant fraction of GOES area-burned estimates smaller than 1km2. The GOES technique employs a sub-pixel algorithm to infer instantaneous fire sizes while the MODIS-based techniques assume a burn area on the order of 1km2 is associated with fire detections. Estimates of total area burned are strongly influenced by large fires and the techniques show more consistency during months when large fires occur.
2. CO emissions are more consistent than area estimates over CONUS. This is a result of significant differences among the models in net CO emission rates per unit area within particular ecosystems and vegetation classes. Visual inspection of ecozone maps suggests largest differences are associated with forested land.
3. Based on a 2006 RAQMS model reanalysis, the RAQMS CO emissions have a low bias ranging from zero to 25% over southeastern CONUS during spring and summer and from zero to 50%

over the Pacific Northwest during summer. Because the NCAR Regional emissions are larger than RAQMS in the Southeast during March, and the NCAR Regional and GOES emissions are larger than RAQMS in the Pacific Northwest and the Southeast during July, we infer that these low biases can likely be diminished by use of other reasonable emissions estimates.

4. Globally, RAQMS has a high bias in CO emissions during 3 of 4 times and locations of large tropical biomass burning, demonstrating an ecosystem dependence within tropical regions. At this time we have not determined whether these biases are associated with area burned, the fuel or combustion estimates, or a combination of factors.

REFERENCES

Andreae, M.O. and P. Merlet (2001), Emission of trace gases and aerosols from biomass burning, Global Biogeochemical Cycles 15 (4), 955–966.

Cofer, W.R., III, J.S. Levine, E.L. Winstead, and B.J. Stocks (1991), Trace gas and particulate emissions from biomass burning in temperate ecosystems, in Global Biomass Burning: Atmospheric, Climatic, and Biospheric Implications, edited by J.S. Levine, pp. 203-208, MIT Press, Cambridge, Mass.

Emmons, L. (2007), National Center for Atmospheric Research, personal communication.

Giglio, L., G. R. van der Werf, J. T. Randerson, G. J. Collatz, and P. Kasibhatla (2006), Global estimation of burned area using MODIS active fire observations, Atmos. Chem. Phys., 6, 957–974.

Giglio, L. (2007), MODIS Collection 4 Active Fire Product User's Guide Version 2.3, available on-line [http://maps.geog.umd.edu/products/MODIS_Fire_Users_Guide_2.3.pdf].

Haines, D.A. (1988), A lower atmospheric severity index for wildland fires, National Weather Digest, 13, 23-27.

Kittaka, C. et al. (2004), A three-dimensional regional modeling study of the impact of clouds on sulfate distributions during TRACE-P, J. Geophys. Res., 109, D15S11, doi:10.1029/2003JD004353.

NASA/University of Maryland (2002), MODIS Active Fire Detections Data set, MODIS Rapid Response Project, NASA/GSFC [producer], University of Maryland, Fire Information for Resource Management System [distributors], available on-line [http://maps.geog.umd.edu].

Olson, J. S. (1983), Carbon in live vegetation of major world ecosystems, ORNL-5862, Environmental Sciences Division Publication No. 1997, Oak Ridge National Laboratory, Oak Ridge, Tennessee.

Pierce, R. B. et al. (2003), Regional Air Quality Modeling System (RAQMS) predictions of the tropospheric ozone budget over east Asia, J. Geophys. Res. 108, 8825, doi:10.1029/2002JD003176.

Pierce, R. B. et al. (2007), Chemical Data Assimilation Estimates of Continental US ozone and Nitrogen budgets during INTEX-A, J. Geophys. Res., in press.

Prins, E. M., C. C. Schmidt, J. M. Feltz, J. S. Reid, D. L. Wesphal, and K. Richardson (2003), A two-year analysis of fire activity in the Western Hemisphere as observed with the GOES Wildfire Automated Biomass Burning Algorithm, 12th Conf. on Satellite Meteorology and Oceanography, Long Beach, CA, Amer. Meteor. Soc., CD-ROM, P2.28.

Soja A.J., Cofer W.R., Shugart H.H., Sukhinin A.I., Stackhouse P.W. Jr., McRae D., and Conard S.G. (2004), Estimating fire emissions and disparities in boreal Siberia (1998 through 2002), J. Geophys. Res., doi:10.1029/2004JD004570.

Soja, A. J. et al. (2007a), A methodology and assessment of estimating area burned in near real time, this issue.

Soja, A. J. et al. (2007b), Description of a ground-based methodology for estimating boreal fire emissions for use in regional- and global-scale transport models, in preparation, 2007.

Tang, Y. et al. (2007), The influence of lateral and top boundary conditions on regional air quality prediction: a multi-scale study coupling regional and global chemical transport models, J. Geophys. Res., in press.

University of Wisconsin (2003), Biomass burning monitoring page at UW-Madison/SSEC/CIMSS, available online at http://cimss.ssec.wisc.edu/goes/burn/abba.html.

van der Werf, G. R., J. T. Randerson, L. Giglio, G. J. Collatz, P. S. Kasibhatla, and A. F. Arellano, Jr. (2006), Interannual variability in global biomass burning emissions from 1997 to 2004, Atmos. Chem. Phys., 6, 3423–3441.

Wiedinmyer. C., B. Quayle, C. Geron, A. Belote, D. McKenzie, X. Zhang, S. O'Neill, and K. K. Wynne (2006), Estimating emissions from fires in North America for air quality modeling, Atmos. Environ., 40, 3419–3432.

Zhang, X. and S. Kondragunta (2006a), Using GOES Instantaneous Fire Sizes as a Proxy for Burned Areas, GOFC/GOLD 2nd Workshop, Germany, 4-6 December.

Zhang, X., and S. Kondragunta (2006b), Estimating forest biomass in the USA using generalized allometric models and MODIS land products, Geophys. Res. Lett., 33, L09402, doi:10.1029/2006GL025879.

Zinke, P.J., A.G. Strangenberger, W.M. Post, W.R. Emanuel, and J.S. Olson (1986), Worldwide Organic Soil Carbon and Nitrogen Data, NDP-018, 134 pp., Oak Ridge National Laboratory, Oak Ridge, Tennessee.

Table 1 Basic characteristics of the 2006 biomass burning emission products used in this study.

	NASA Global (RAQMS)	NCAR Global (MOZART)	NCAR Regional	NOAA GOES
Domain	Global	Global	North+Central America	CONUS
Satellite Fire Detection	MODIS Rapid Response	MODIS Climate Modeling Grid	MODIS Rapid Response	GOES processed half-hourly
2006 Dates of Coverage	Feb 1 – Oct 15	Jan 1 – Dec 31	Jan 1 – Dec 31	Mar 1 – Sep30
Horizontal Resolution	1 deg x 1 deg	1 deg x 1 deg	1 km (MODIS nadir pixel size)	4 km (GOES nadir pixel size)
Temporal Resolution	Daily	8-days	Daily	Daily
Species available in this intercomparison	CO, NO, area-burned	CO, NO, CO2, CH4, PM2.5, area-burned	CO, CO2, CH4, PM2.5, VOC, NOx, area-burned	CO, area-burned
Other species typically produced	C; other species (NMHC, aerosol) calculated from C	Other species calculated from CO2	PM10, HCN, CH3CN, NH3, SO2, Hg	PM2.5, CH4

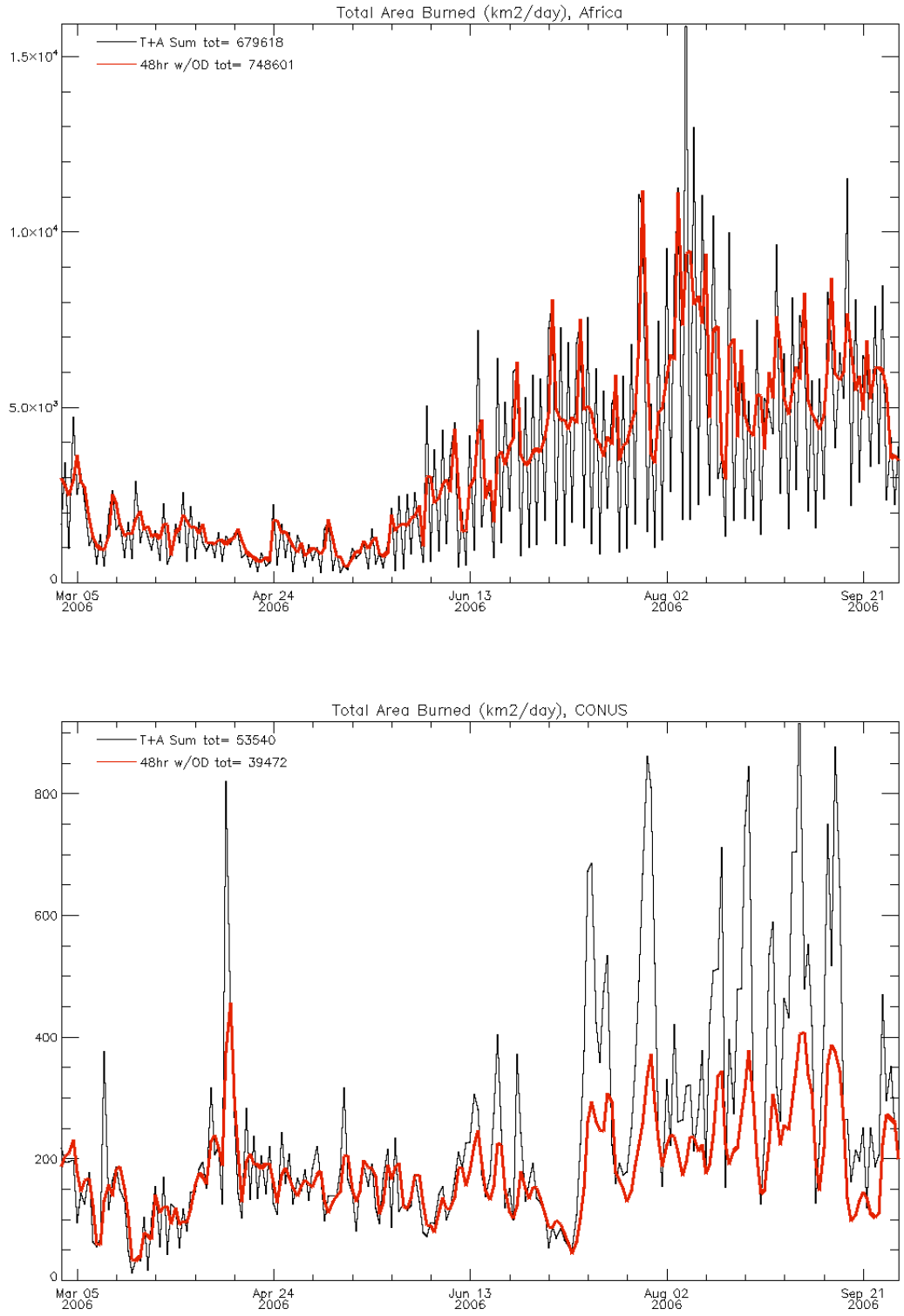

Figure 1 Time series of daily area burned estimates integrated over Africa and the continental US (CONUS) from March 1 through September 30, 2006. Shown are area estimates resulting from summing all Terra and Aqua fire counts during a 24 hour period (black line) and from the current technique (red line).

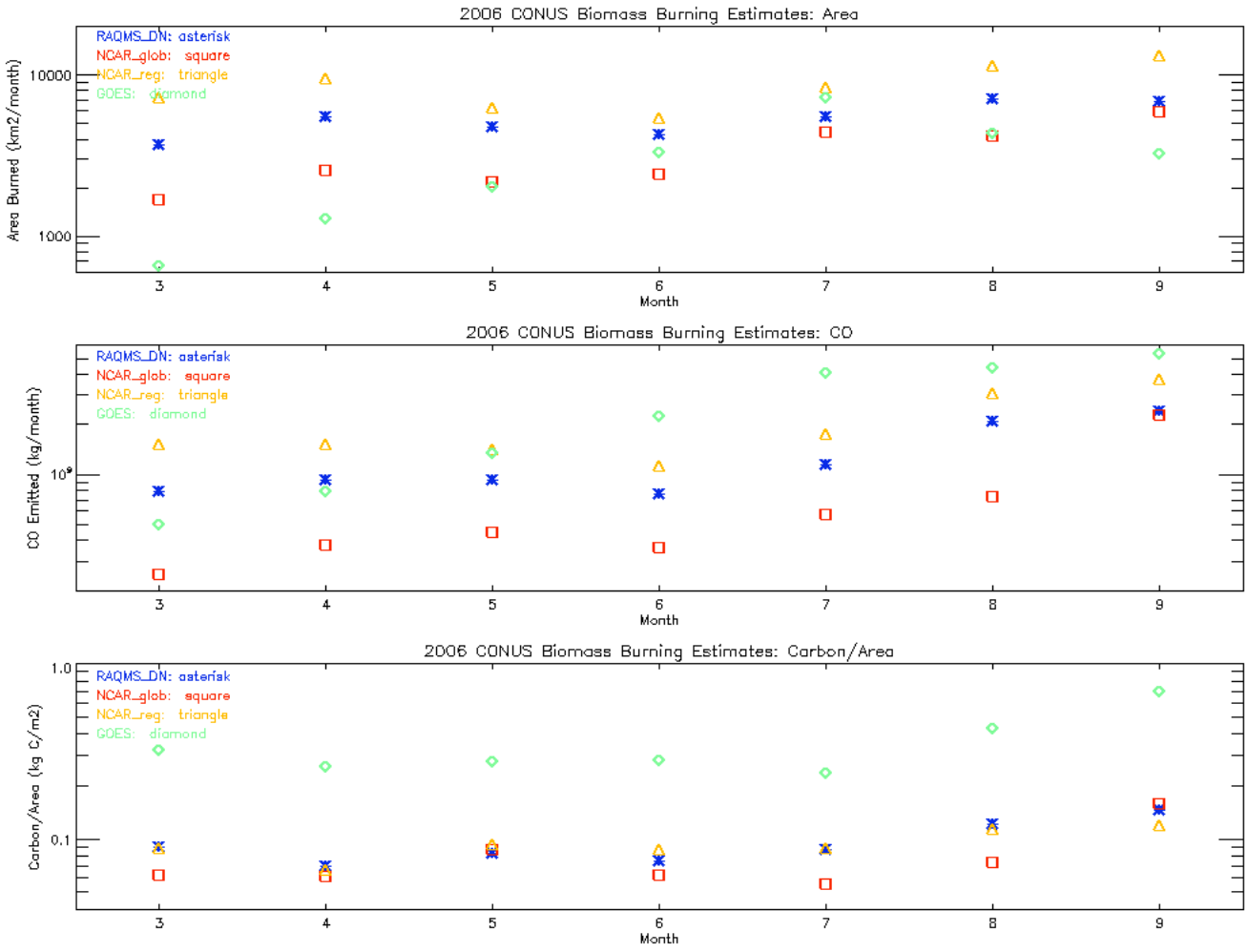

Figure 2 Monthly biomass burning estimates integrated over the continental United States during 2006. Top panel: area burned. Middle panel: CO emission. Bottom panel: net emission efficiency, Carbon/area.

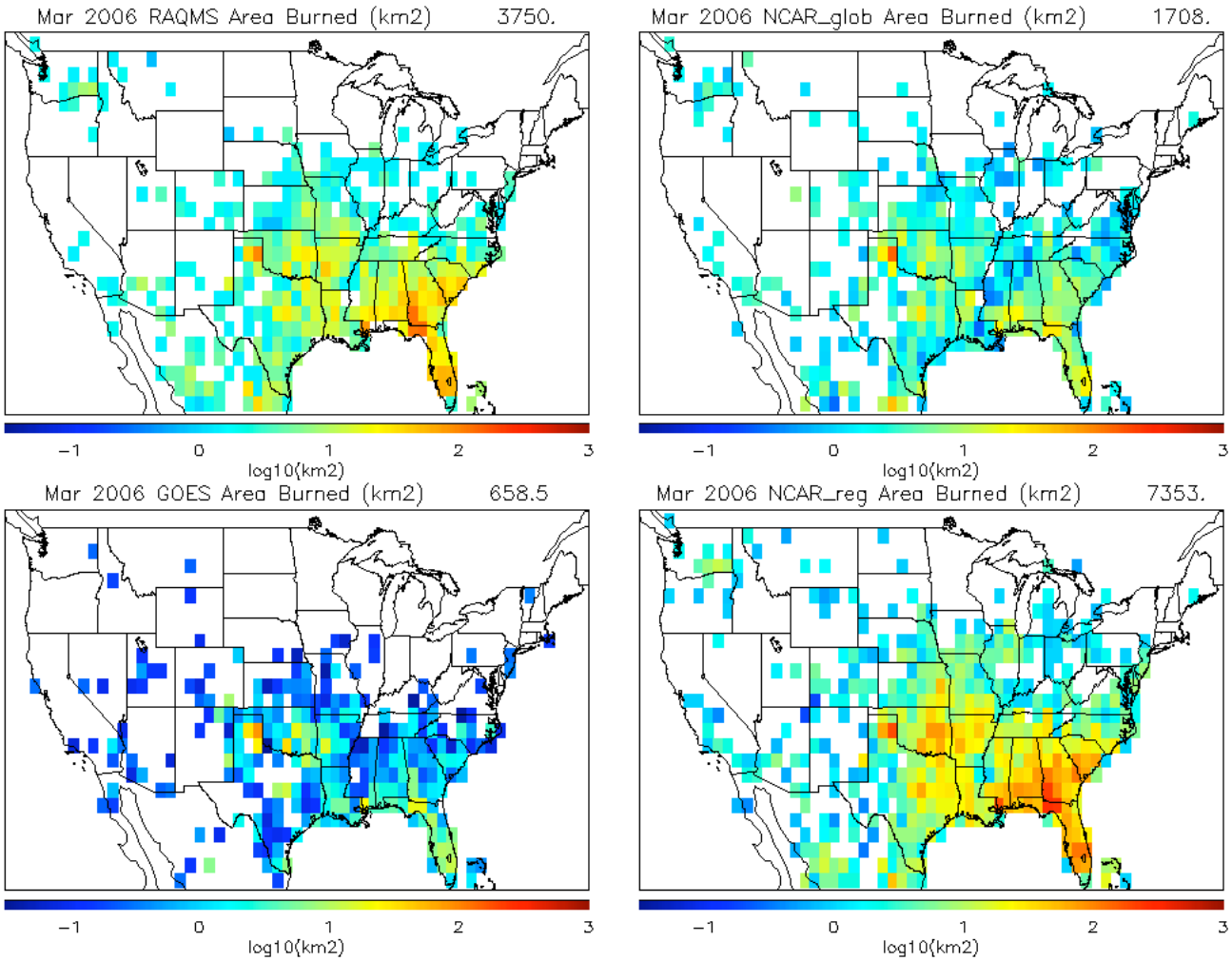

Figure 3 Maps of area burned estimates from each technique during March 2006.

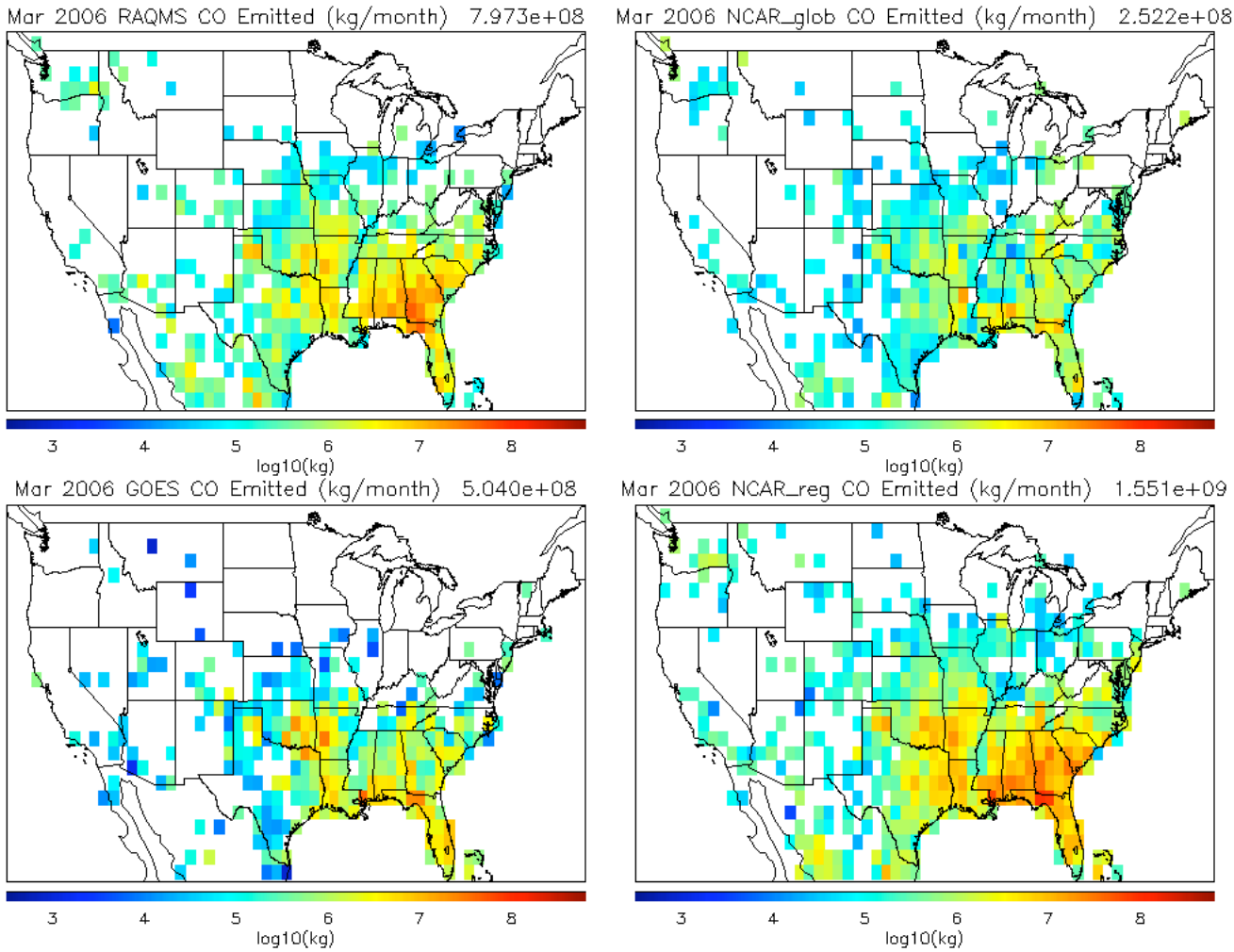

Figure 4 Maps of Carbon Monoxide emission estimates from each technique during March 2006.

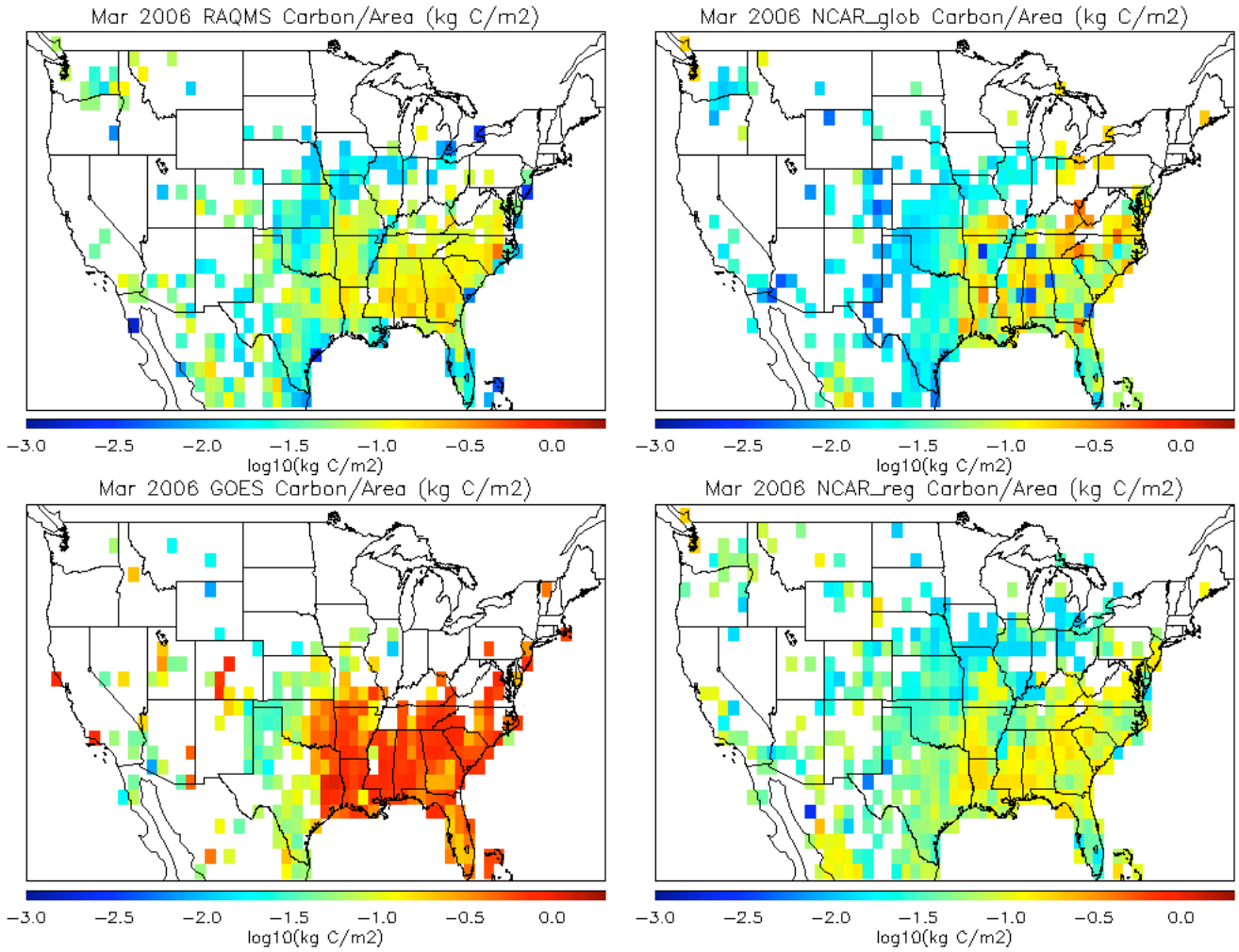

Figure 5 Maps of the ratio of Carbon emitted to area burned from each technique during March 2006.

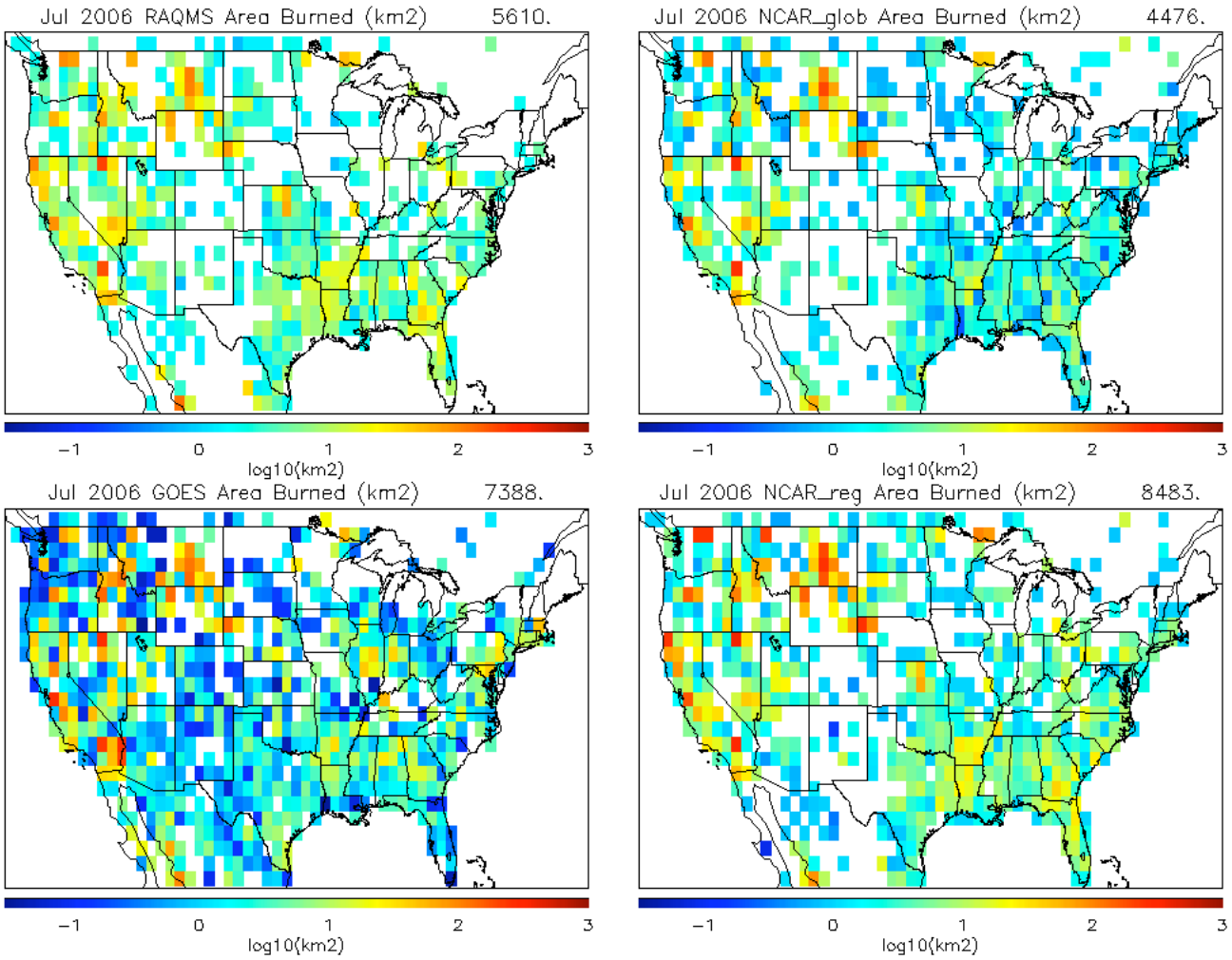

Figure 6 Maps of area burned estimates from each technique during July 2006.

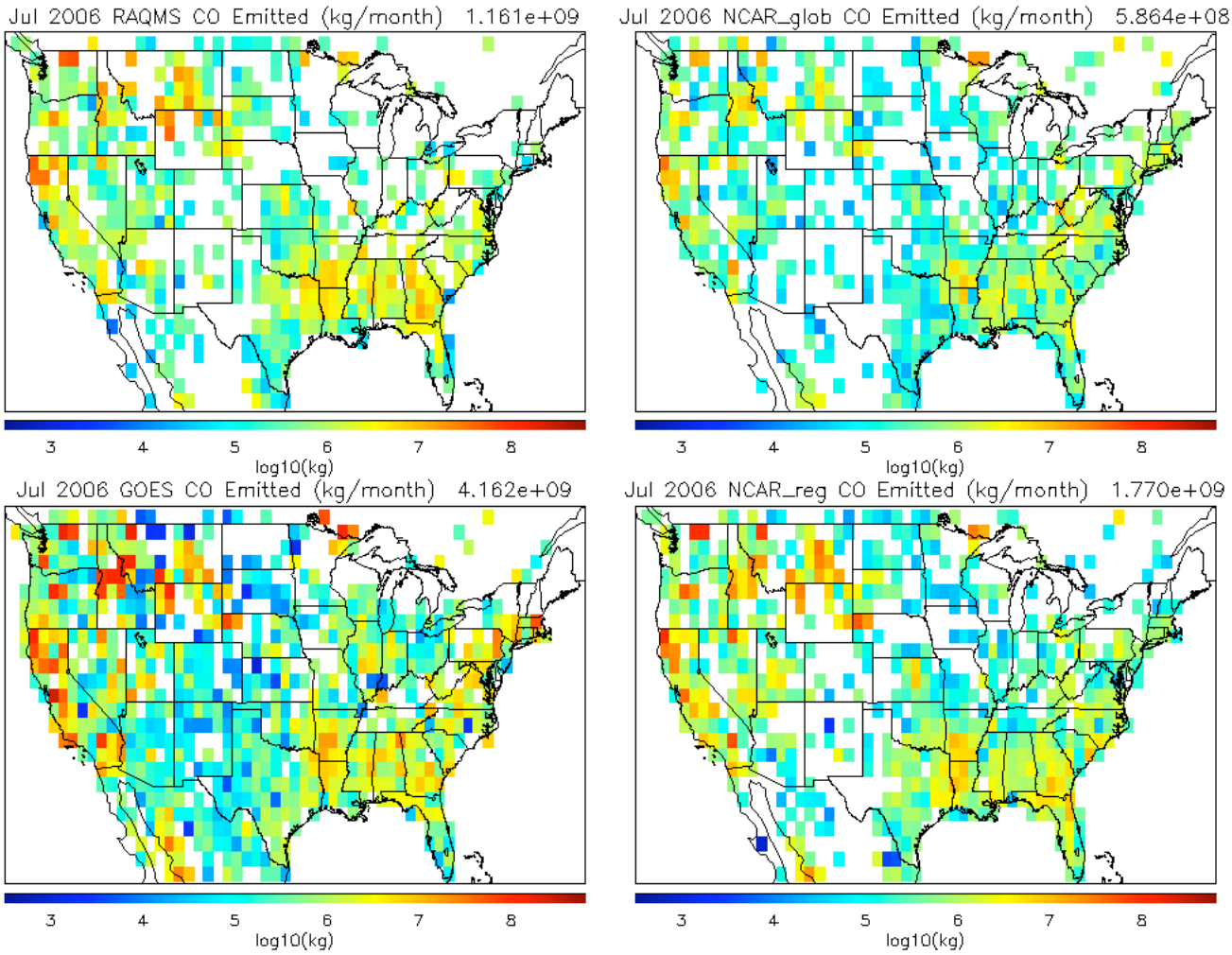

Figure 7 Maps of Carbon Monoxide emission estimates from each technique during July 2006.

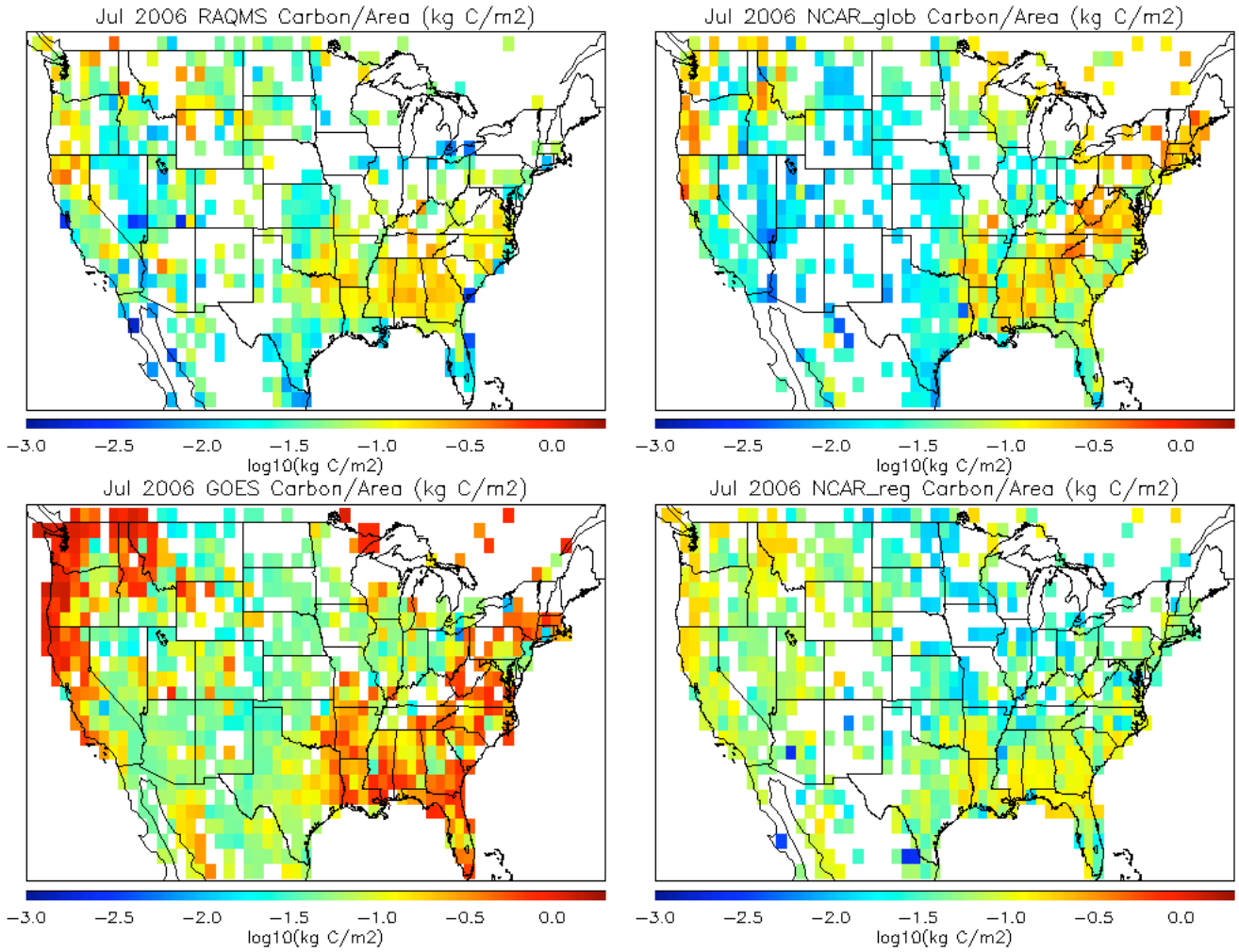

Figure 8 Maps of the ratio of Carbon emitted to area burned from each technique during July 2006.

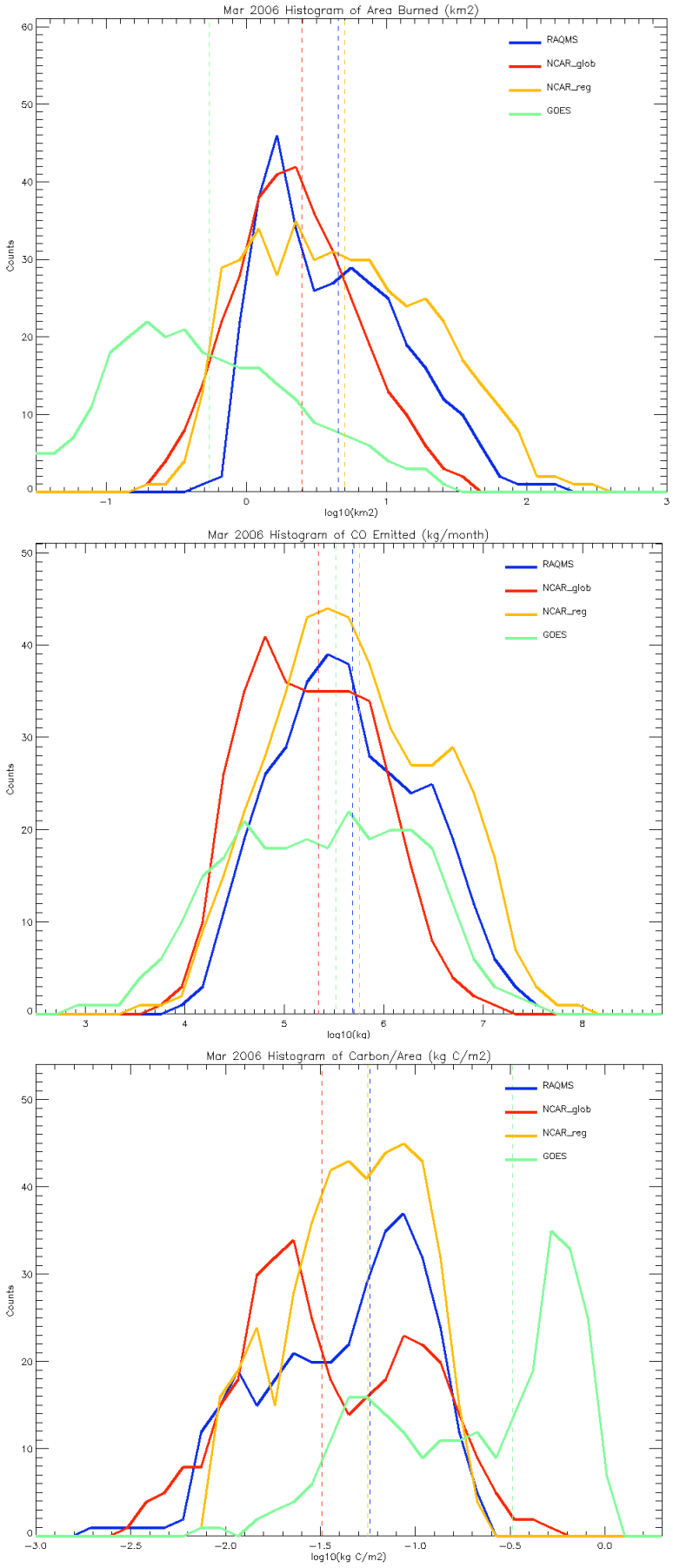

Figure 9 Histograms of area burned, CO emitted, and net Carbon emission efficiency during March 2006. Blue: RAQMS. Red: NCAR Global. Orange: NCAR Regional. Green: GOES.

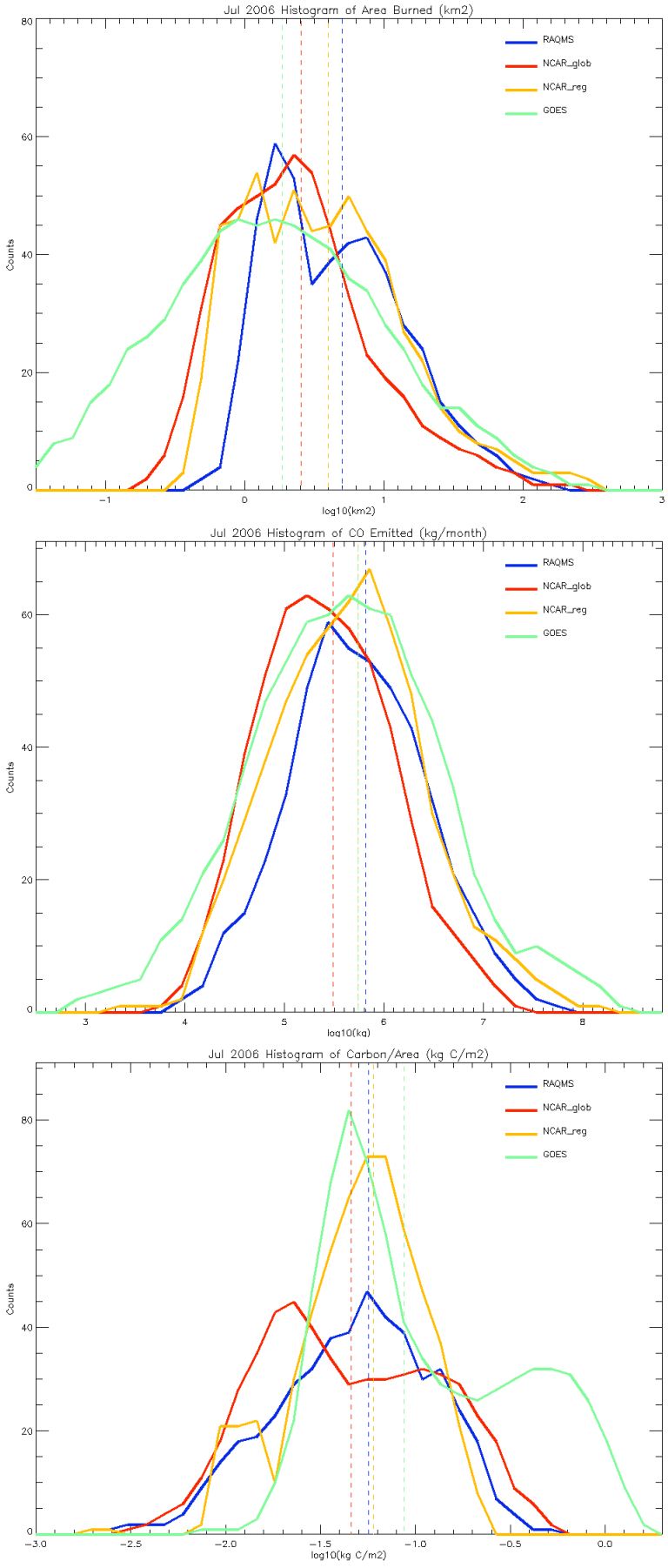

Figure 10 Histograms of area burned, CO emitted, and net Carbon emission efficiency during July 2006. Blue: RAQMS. Red: NCAR Global. Orange: NCAR Regional. Green: GOES.

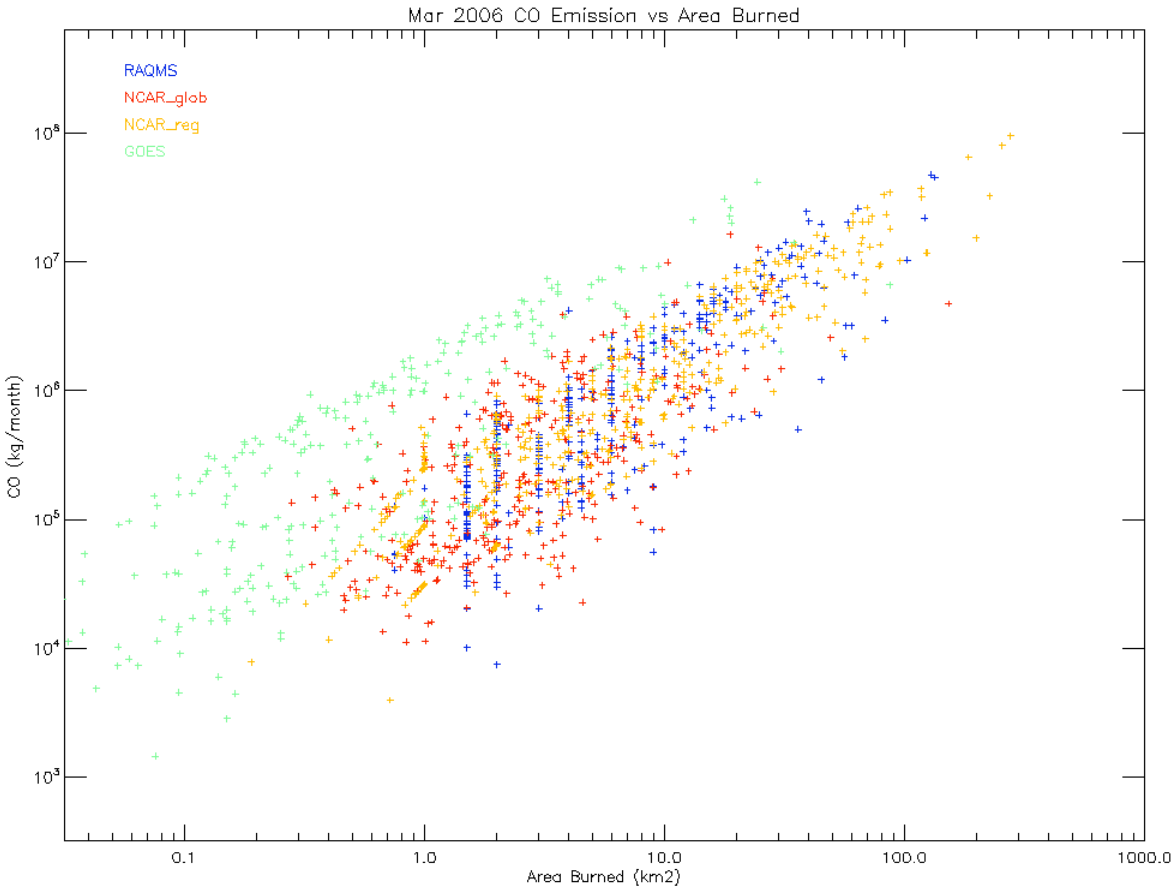

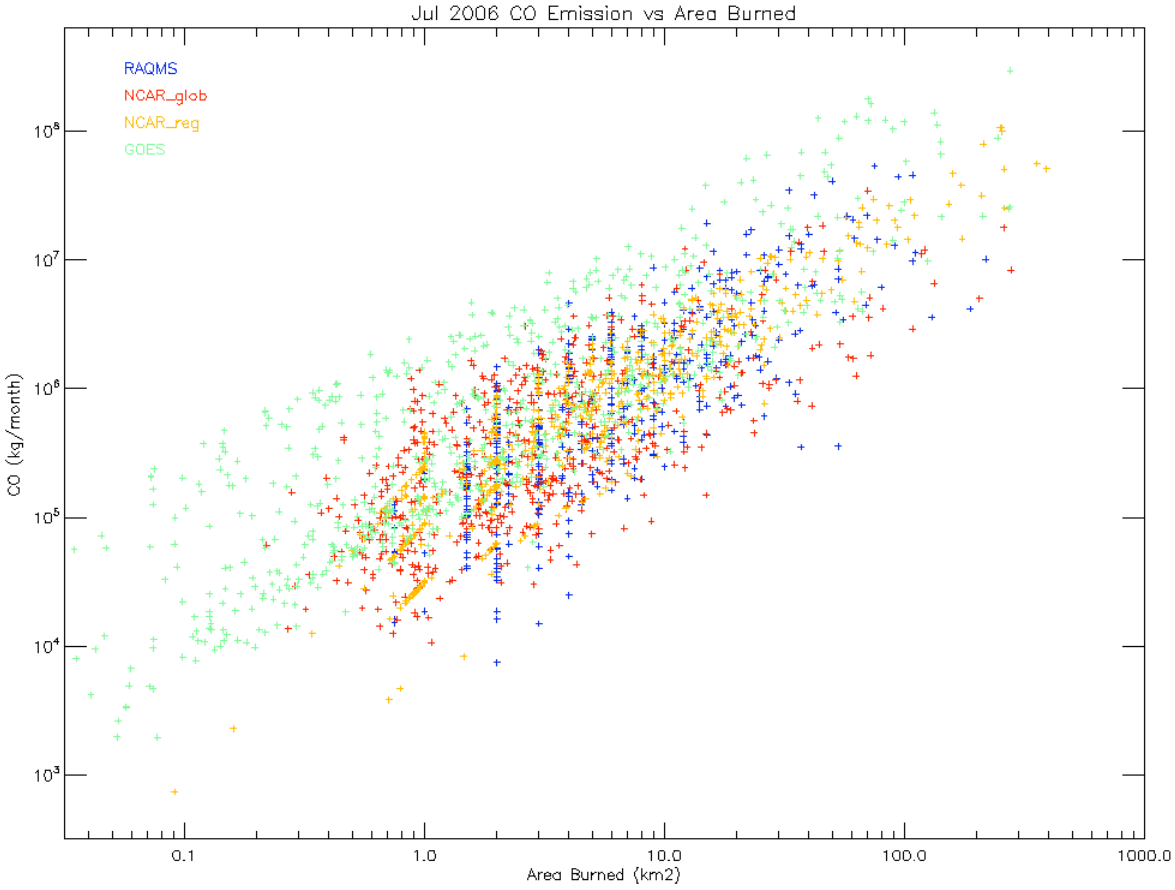

Figure 11 Scatter plots of CO emitted versus area burned during March and July 2006. Blue: RAQMS. Red: NCAR Global. Orange: NCAR Regional. Green: GOES.

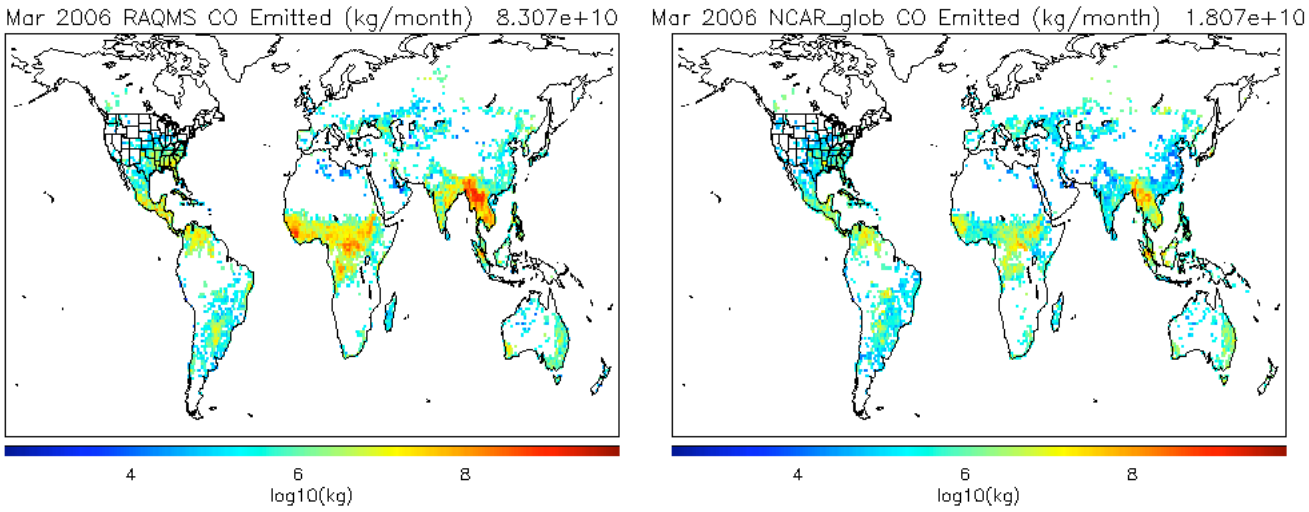

Figure 12 March 2006 global biomass burning CO emissions from RAQMS and NCAR Global techniques.

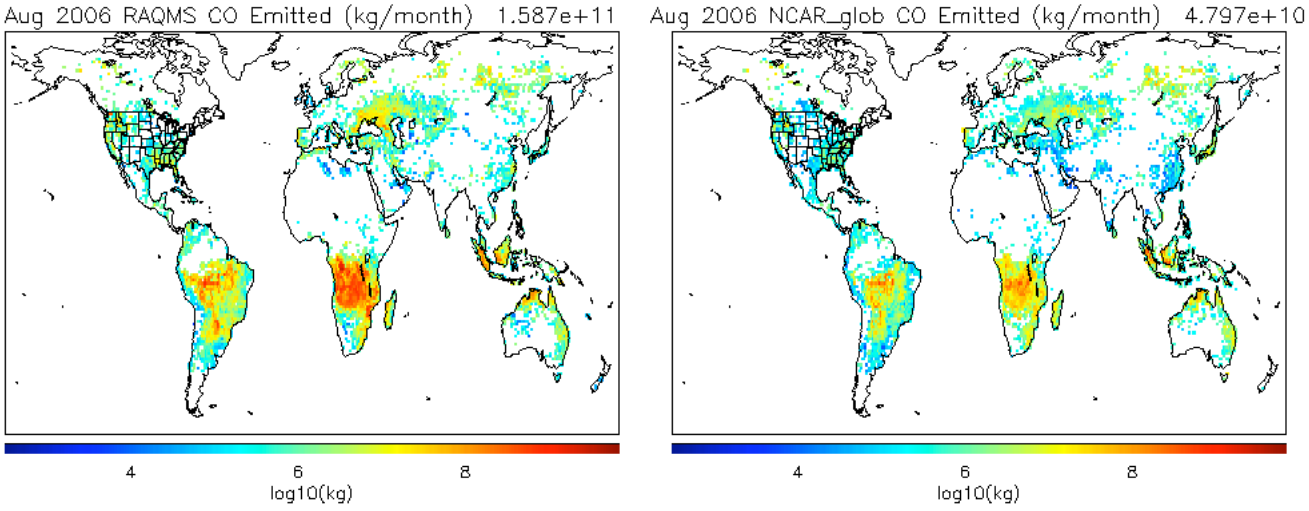

Figure 13 Same as Figure 12 except for August 2006.

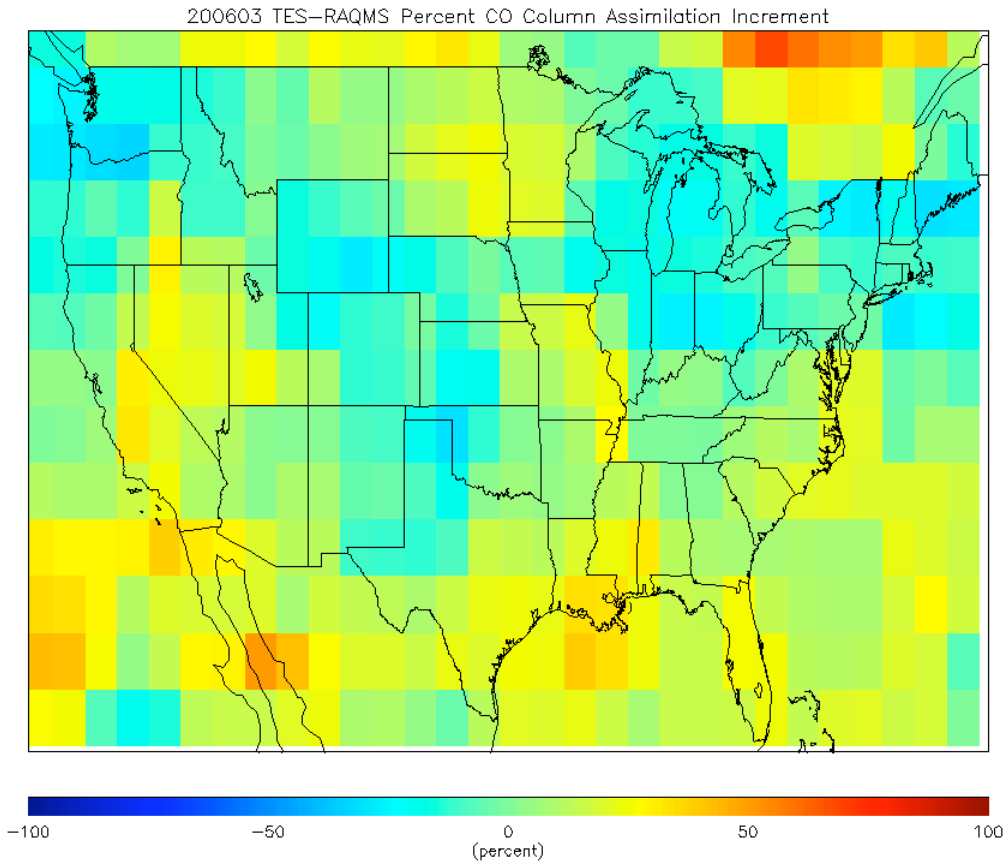

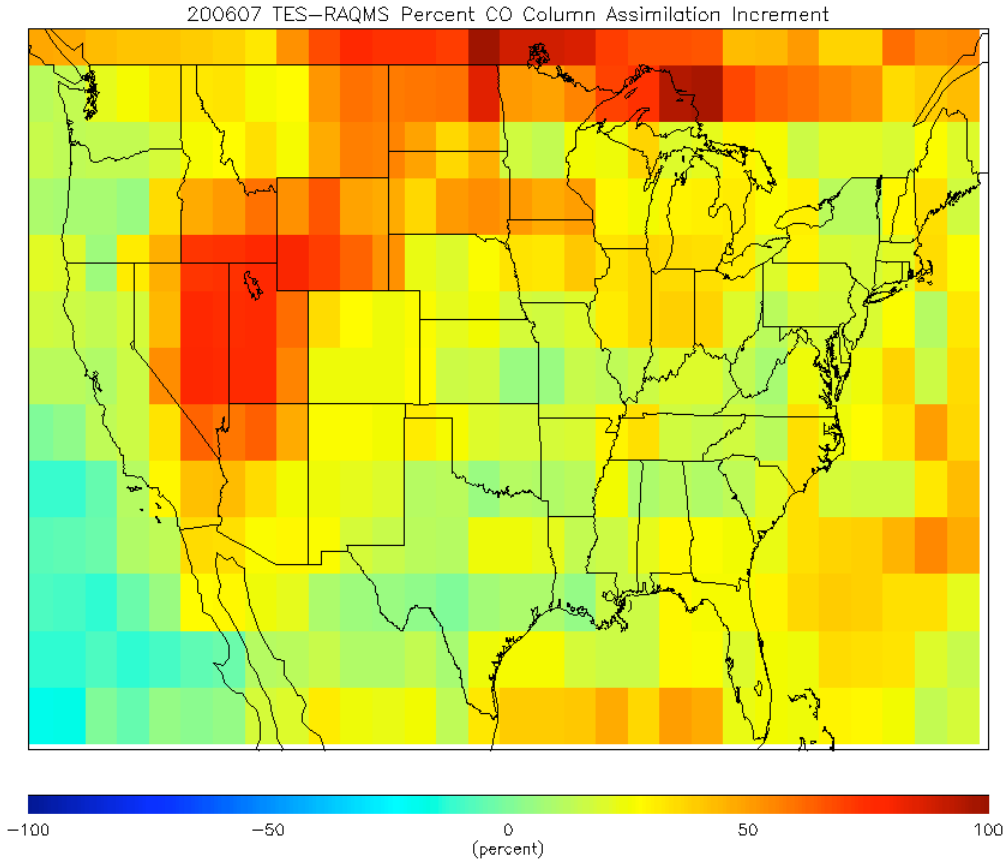

Figure 14 TES-RAQMS carbon monoxide assimilation increments, expressed as percentages of the total column amounts, accumulated over March and July 2006.

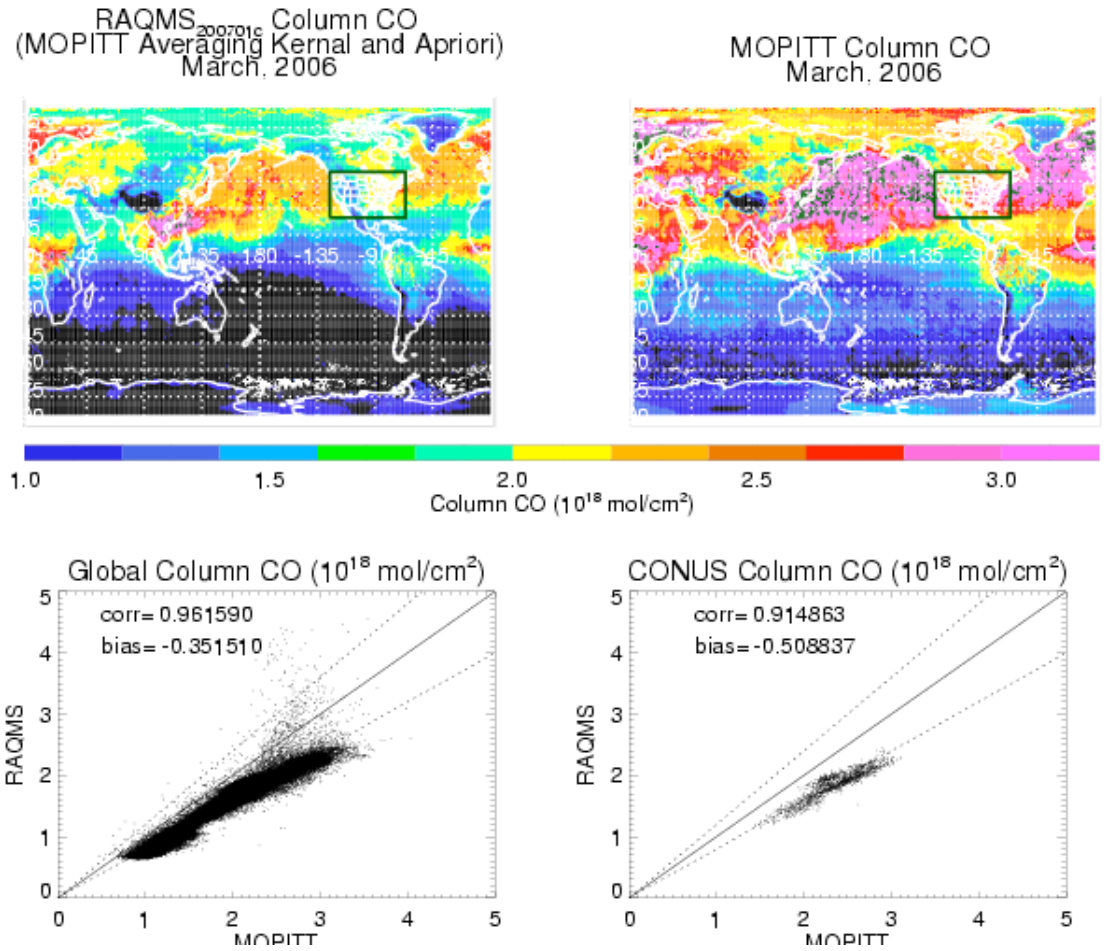

Figure 15 Comparison of column CO amounts from the RAQMS model and MOPITT observations during March 2006. Scatter plots show mean statistics over global (bottom left) and CONUS (bottom right) domains.

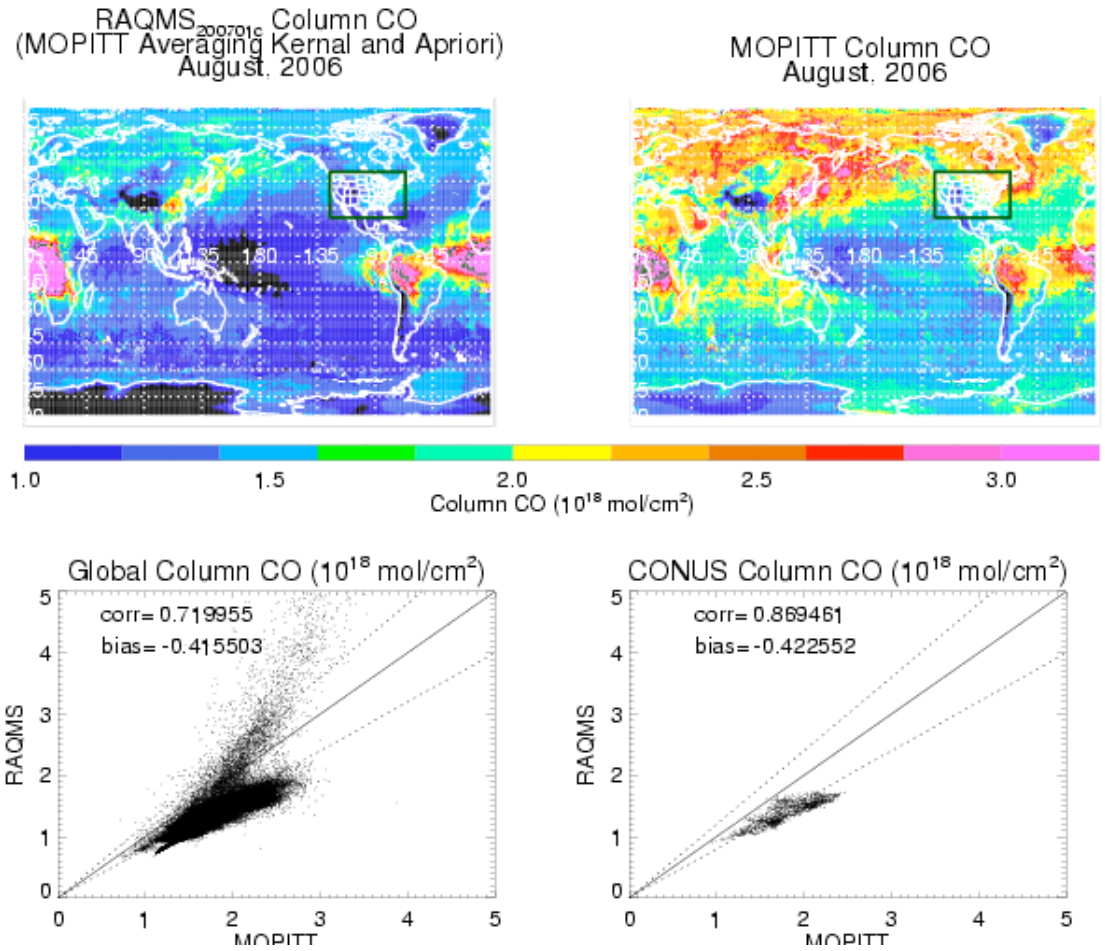

Figure 16 Same as Figure 15 except for August 2006.